

Deep learning virtual colorization overcoming chromatic aberrations in singlet lens microscopy

Cite as: APL Photonics 6, 031301 (2021); <https://doi.org/10.1063/5.0039206>

Submitted: 01 December 2020 • Accepted: 09 February 2021 • Published Online: 01 March 2021

 Yinxu Bian, Yannan Jiang, Yuran Huang, et al.

COLLECTIONS

Paper published as part of the special topic on [Coronavirus and Photonics](#)



View Online



Export Citation



CrossMark

ARTICLES YOU MAY BE INTERESTED IN

[Current challenges and solutions of super-resolution structured illumination microscopy](#)

APL Photonics 6, 020901 (2021); <https://doi.org/10.1063/5.0038065>

[Perspectives on advances in high-capacity, free-space communications using multiplexing of orbital-angular-momentum beams](#)

APL Photonics 6, 030901 (2021); <https://doi.org/10.1063/5.0031230>

[Photonic band structure design using persistent homology](#)

APL Photonics 6, 030802 (2021); <https://doi.org/10.1063/5.0041084>

Learn more and submit

APL Photonics

Applications now open for the
Early Career Editorial Advisory Board

Deep learning virtual colorization overcoming chromatic aberrations in singlet lens microscopy

Cite as: APL Photon. 6, 031301 (2021); doi: 10.1063/5.0039206
Submitted: 1 December 2020 • Accepted: 9 February 2021 •
Published Online: 1 March 2021



Yinxu Bian,¹  Yannan Jiang,² Yuran Huang,^{3,4} Xiaofei Yang,⁵ Weijie Deng,^{6,7} Hua Shen,^{1,8} Renbing Shen,^{2,a)} and Cuifang Kuang^{3,4,a)}

AFFILIATIONS

¹School of Electronic and Optical Engineering, Nanjing University of Science and Technology, Nanjing 210094, China

²Department of General Surgery, The Affiliated Suzhou Hospital of Nanjing Medical University, Suzhou Municipal Hospital, Suzhou 215002, China

³State Key Laboratory of Modern Optical Instrumentation, Zhejiang University, Hangzhou 310027, China

⁴College of Optical Science and Engineering, Zhejiang University, Hangzhou 310027, China

⁵School of Optoelectronic Science and Engineering & Collaborative Innovation Center of Suzhou Nano Science and Technology, Soochow University, Suzhou 215006, China

⁶Changchun Institute of Optics, Fine Mechanics and Physics, Chinese Academy of Sciences, Changchun 130033, China

⁷Key Laboratory of Optical System Advanced Manufacturing Technology, Chinese Academy of Sciences, Changchun 130033, China

⁸Department of Material Science and Engineering, University of California Los Angeles, Los Angeles, California 90095, USA

Note: This paper is part of the APL Photonics Special Topic on Coronavirus and Photonics.

^{a)} **Authors to whom correspondence should be addressed:** 13862031461@qq.com and cfkuang@zju.edu.cn

ABSTRACT

Singlet lenses are free from precise assembling, aligning, and testing, which are helpful for the development of portable and low-cost microscopes. However, balancing the spectrum dispersion or chromatic aberrations using a singlet lens made of one material is difficult. Here, a novel method combining singlet lens microscopy and computational imaging, which is based on deep learning image-style-transfer algorithms, is proposed to overcome this problem in clinical pathological slide microscopy. In this manuscript, a singlet aspheric lens is used, which has a high cut-off frequency and linear signal properties. Enhanced by a trained deep learning network, it is easy to transfer the monochromatic gray-scale microscopy picture to a colorful microscopy picture, with only one single-shot recording by a monochromatic CMOS image sensor. By experiments, data analysis, and discussions, it is proved that our proposed virtual colorization microscope imaging method is effective for H&E stained tumor tissue slides in singlet microscopy. It is believable that the computational virtual colorization method for singlet microscopes would promote the low-cost and portable singlet microscopy development in medical pathological label staining observing (e.g., H&E staining, Gram staining, and fluorescent labeling) biomedical research.

© 2021 Author(s). All article content, except where otherwise noted, is licensed under a Creative Commons Attribution (CC BY) license (<http://creativecommons.org/licenses/by/4.0/>). <https://doi.org/10.1063/5.0039206>

INTRODUCTION

Commercial microscope objective lenses, cell-phone camera lenses, and other imaging lenses are cheap due to the mass industrial production. However, as they consist of multiple pieces of lenses, the cost mainly focuses on the mounting and testing of lenses. In contrast, singlet lenses are free from precise assembling, aligning,

and testing.¹⁻³ The singlet lenses can reduce time, money, and labor cost extensively, resulting in a further price and integration revolution of imaging devices. Many researchers have designed and fabricated to achieve singlet imaging/microscopy, including the graded index (GRIN) lens,^{4,5} metalens^{6,7} based on a metasurface and meta-material, diffractive optical element,^{8,9} non-rotational symmetric freeform surface,¹⁻³ and other aspheric lenses. The GRIN lens can

eliminate spherical aberrations well, while it cannot overcome the off-axial aberrations at a large field of view (FOV). The metalens is thin and light, while it requires time-consuming fabrications and has difficulties in surface measurements. The metasurfaces are usually fabricated by Electron Beam Lithography (EBL) and Focused-Ion-Beam (FIB) etching, which greatly increase the manufacturing costs. These limitations restrict the usage of metalenses. For non-rotational symmetric freeform surfaces, they are difficult to design,

mathematically describe, and test. Besides, colorfully imaging these metalenses and non-rotational symmetric freeform surfaces, made of one material, with single-shot recording is difficult.

In this manuscript, we propose a method, combining deep learning virtual colorization and designed singlet lens, to achieve large FOV singlet colorful microscopy. We use a custom-designed singlet aspheric lens as the objective lens. The custom-designed singlet aspheric lens aims to obtain a high cut-off spatial frequency

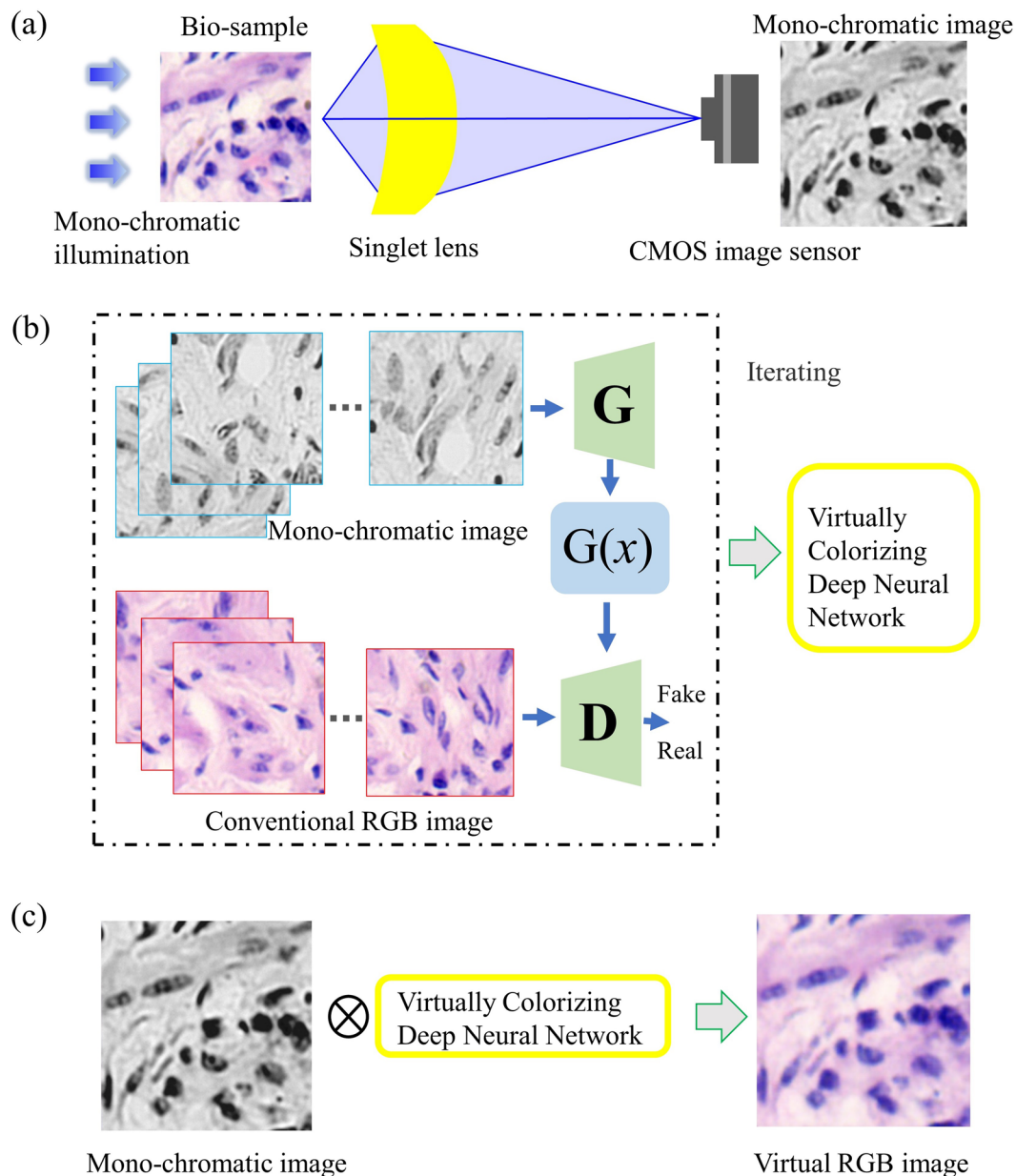


FIG. 1. An overview to achieve the singlet microscopy colorization. (a) Schematic of a singlet microscopy system. (b) Virtually colorizing deep learning training stage. G means the “generator,” $G(x)$ means the generated image by the “generator,” and D means the “discriminator.” (c) Practical transferring stage: a monochromatic image is convolved with the trained “virtually colorizing deep neural network” in (b) directly.

and keep the imaging system with linear signal properties. The high cut-off frequency is due to the fact that the computational imaging cannot generate new high-frequency information and can only optimize the imaging performance based on the originally recorded images. The reason for the use of linear imaging system is that the computational imaging can achieve the best results under a linear system. By computational image-style-transfer methods based on deep learning, we could achieve colorful microscopy with a single-shot digital recording. Different from natural scene photographs, scenes of microscopy images are simpler^{10–22} because the biosamples, e.g., pathological tissue sections and cells, are usually stained with a gold-standard dye and fluorescence label. The chemical dyes and fluorescence labels are always with limited artificial colors. For example, the pathological tissue sections samples used in this manuscript are hematoxylin and eosin (H&E) stained, which is one of the widely used tissue stains in histology and medical diagnosis. After H&E staining, cell nuclei will appear purplish-blue, while the cellular matrix and cytoplasm will appear pink by the H&E stain.^{15–19} Based on the two limited artificial colors, all structures and details of pathological tissue section samples appear as different

shades and hues, which results in easy observation. Thus, we propose the deep learning image-style-transfer method to translate a chromatic grayscale image to a colorful image. Obviously, we provide a new aspect to achieve colorful microscopy method for all imaging systems with spectrum dispersion/chromatic aberrations. Our proposed ideas and methods could be introduced into metalens and designing of other lenses. The virtually colorizing computational image-style-transfer method could be combined with the all imaging system with chromatic aberrations.

Figure 1 shows the overview to achieve the singlet microscopy colorization. Figure 1(a) shows the schematic of a singlet microscopy experimental setup. It is very simple and constructed easily. The singlet lens is presented in Fig. 2. Also, our singlet lens could be replaced by a meta-surface lens and other singlet lens. In Fig. 1(a), the pathological tissue slide is illuminated by a mono-chromatic light, which could be a cheap blue (B) light-emitting diode (LED), green (G) LED, and red (R) LED. The slide is also at the object plane of the singlet aspheric lens, and a mono-CMOS image sensor (MTR3CMOS2000KMA, TOUPVIEW, China) is at the conjunct imaging plane of the singlet aspheric lens. The LED, biosample slide,

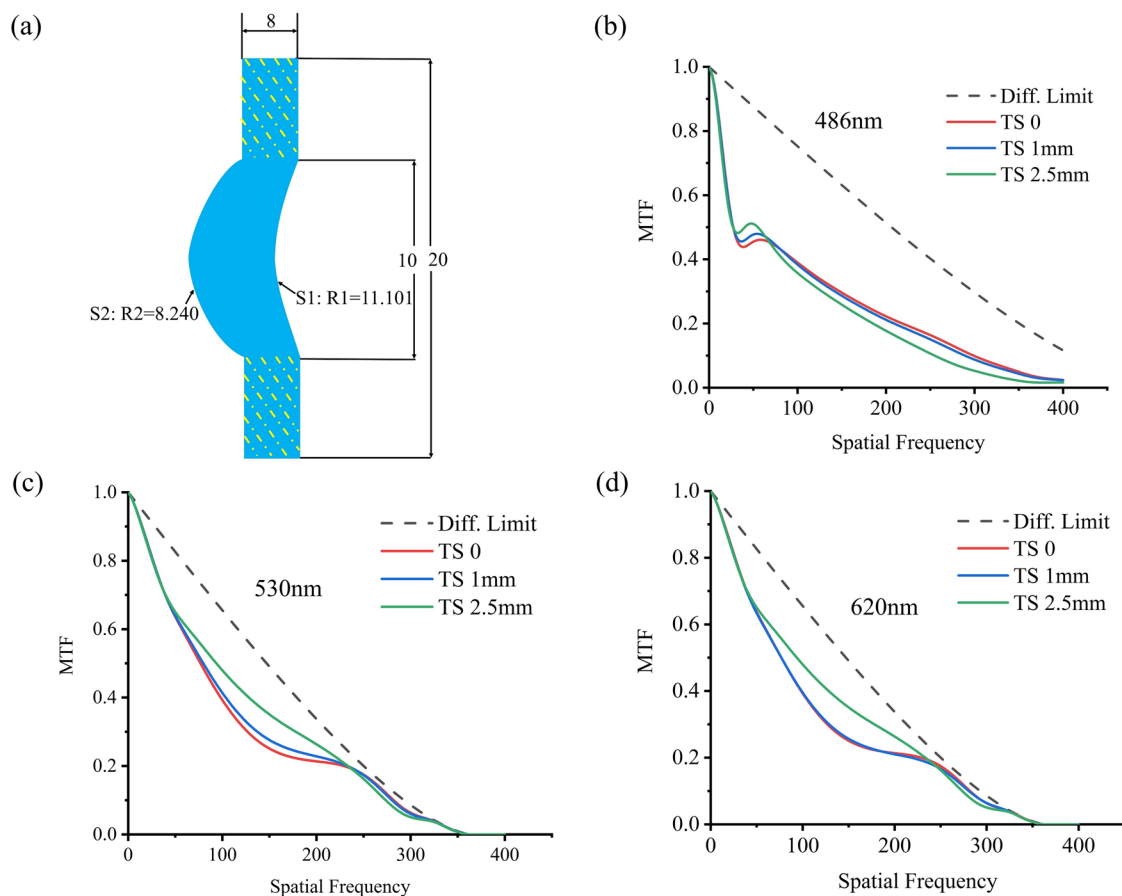


FIG. 2. Custom-designed singlet aspheric lens and its MTF curves. (a) Our singlet lens made of E48R. (b) MTF curves across the FOV of 0 mm–2.5 mm at the wavelength of 486 nm. (c) MTF curves across the FOV of 0 mm–2.5 mm at the wavelength of 530 nm. (d) MTF curves across the FOV of 0 mm–2.5 mm at the wavelength of 620 nm. (b)–(d) all show that the singlet aspheric lens in (a) has a high cut-off frequency under a chromatic wavelength illumination and good linear signal properties.

singlet aspheric lens, and mono-CMOS image sensor are all along the optical axis. When the monochromatic light is in the “ON” state, a grayscale image is recorded by the mono-CMOS image sensor. Figure 1(b) contains two data processing stages, i.e., the deep learning training stage (the blue dot line arrow) and the practical transferring stage (the red dotted line arrow). In the deep learning training stage, the input data are the grayscale monochromatic images and the conventional RGB microscopy images. The conventional RGB microscopy images are collected by using the research-level commercial microscope (NIB900, NOVEL, China) and a RGB CMOS image sensor (MTR3CMOS2000KPA, TOUPVIEW, China). The virtual colorization kernel between the grayscale monochromatic images and the RGB colorful images would be iteratively trained by a style-transfer generative adversarial network (GAN),^{10–22} which is explained in Fig. 3. Once the virtual colorization kernel is obtained, in practical use of the stage in Figs. 1(c) and 1(a), the grayscale singlet microscopy image would be translated into a colorful image after convoluted by the trained virtual colorization deep neural network.

SINGLET LENS

The singlet lens and its modulation transfer function (MTF) curves are presented in Fig. 2. The singlet lens consists of two even aspheric surfaces, which can be expressed by the following equation:²³

$$z = \frac{cr^2}{1 + \sqrt{1 - (1+k)c^2r^2}} + \alpha_1 r^2 + \alpha_2 r^4 + \alpha_3 r^6 + \dots + \alpha_7 r^{14}, \quad (1)$$

where c is the curvature ($1/R$), k is the aspheric coefficient, and α are high order terms coefficients. The first aspheric surface, i.e., the parameters of S1 and S2 are presented in Table I. The lens material is the optics cyclic olefin polymer of E48R (ZEON, JAPAN) and it is manufactured by Nanjing University of Science and Technology (NUST).

The designed objective working distance is 27 mm, and the conjugate imaging working distance depends on the illumination wavelength as the axial chromatic aberration/spectrum dispersions, i.e., 161.7 mm under the blue LED illumination, 175.7 mm under the

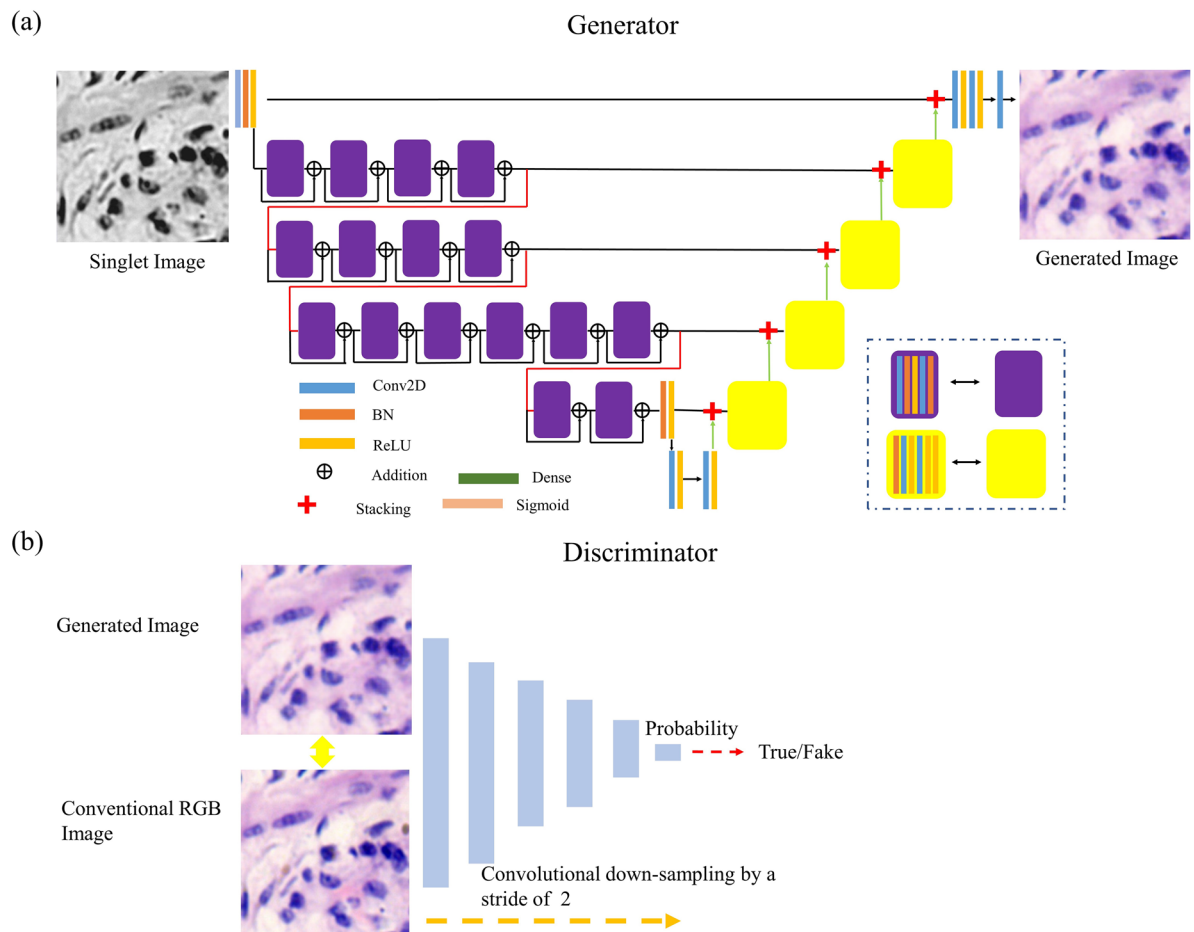


FIG. 3. Deep learning virtually colorizing GAN frameworks. (a) Generator: a designed U-NET-like deep convolution neural network. (b) Discriminator: a convolution neural network to calculate a probability, distinguishing “true” or “fake” image data.

TABLE I. Surface parameters of S1 and S2.

	R	k	α_2	α_3	α_4	α_5	α_6	α_7
S1	8.240	-1	1.864×10^{-4}	1.011×10^{-5}	-8.274×10^{-7}	4.675×10^{-8}	-1.316×10^{-9}	1.443×10^{-11}
S2	11.101	-1	6.558×10^{-4}	-7.207×10^{-5}	3.043×10^{-5}	-4.466×10^{-6}	2.971×10^{-7}	-7.36×10^{-9}

green LED illumination, and 181.7 mm under the red LED illumination. Figure 2(b) shows the MTF curves across the objective FOV of 0 mm–2.5 mm at the wavelength of 486 nm, Fig. 2(c) shows the MTF curves across the objective FOV of 0 mm–2.5 mm at the wavelength of 530 nm, and Fig. 2(d) shows the MTF curves across the objective FOV of 0 mm–2.5 mm at the wavelength of 620 nm. In Figs. 2(b)–2(d), the MTF curves show that our singlet aspheric lens keeps good linear signal properties across the objective FOV of 0 mm–2.5 mm under a chromatic wavelength illumination. Our singlet aspheric lens has a high cut-off frequency under a chromatic wavelength illumination, which is up to 350 lp/mm. These good linear signal properties help greatly for the computational imaging algorithms.

DEEP LEARNING VIRTUALLY COLORIZING

We trained the virtual colorization kernels three times under the blue LED illumination, the green LED illumination, and the red LED illumination. Here, we state the process of deep learning virtually colorizing algorithms using the example under the blue LED illumination. We are not the first to apply the GANs methods to transfer the image style in microscopy. Prior and concurrent works have done so. Our frameworks and data differ greatly in the H&E staining singlet microscopy applications. In algorithm details, we also designed a “U-Net”-like generator network architecture. Before transferring the image style, we used a deep learning deconvolution method to improve the resolution and image contrast.²³ In other image style transfer (Refs. 24–26), such as photograph-to-comics, photograph-to-painting, and day-to-night, the visual feelings are focused, while the texture details are not important. However, in biomedical observation, we hope to keep the image texture and high-resolution-content features in the virtually colorized images. Thus, we add a mass of a direct skip connection in the “U-NET”-like generator network. In this network, the generator would strongly keep the high-resolution-content features of the original grayscale images. Even in the worst deep learning training, the generator should return the original input. The loss function contains two aims, which are similar to Refs. 13, 14, and 20: one is to achieve the style transferring and the other is to keep the high-resolution-content features. In computational environments, the deep learning virtual colorization is processed on a desktop computer, which has a Windows 10 operating system (Microsoft), a Core i7-7700K CPU @ 4.2 GHz (Intel), 64 GB of RAM, and dual GeForce GTX 1080Ti GPUs (NVIDIA). The GAN is constructed by using TensorFlow (TF) framework version 2.1 and Python version 3.7. In GAN deep learning, 1024 pairs of images are for training and 256 pairs of images are for testing. Each image is with the size of 256×256 pixels² in the format of “JPEG” (24 Bit Depth). In the network framework, the batch size is 4, the learning rate is 0.0002, and the epochs are 10 000. The deep training

costs ~20 h, while for practical usage, the virtually colorizing time is ~7 ms.

EXPERIMENTS

The pathological tumor tissue slides were obtained from the Suzhou Municipal Hospital (SMH), which were prepared from existing specimens and followed the basic clinical information de-identification. All processing of tumor biosamples has been approved and supervised by the Medical Ethics Committee of SHM. These tumor tissue biosamples were baked at 68 °C for 30 min. Then, they were deparaffinized through xylene and absolute and 95% alcohols to distilled water. After preparation, the sections were dyed with hematoxylin and eosin in turn, dehydrated through graded ethanol solutions, and cleared with xylene. Finally, the H&E stained slides were sealed with a half drop of neutral resin gum and covered with a coverslip. In the singlet data collection process, the image data are recorded at three wavelength LEDs, respectively. The blue LED is with the dominant wavelength of 485 nm and the full width at half maximum (FWHM) of ~40 nm. The green LED is with the dominant wavelength of 530 nm and the FWHM of ~20 nm. The red LED is with the dominant wavelength of 620 nm and the FWHM of ~30 nm. The pathological tissue slide is put at the objective working length of 27 mm. When the blue LED illuminates, the monochromatic CMOS image sensor is at the conjugate imaging position of 161.7 mm and a set of blue LED illuminating images are recorded. When the green LED illuminates, the monochromatic CMOS image sensor is moved to 175.7 mm and a set of green LED illuminating images are recorded. Finally, when the red LED illuminates, the monochromatic CMOS image sensor is moved to 181.7 mm and a set of red LED illuminating images are recorded. These singlet microscopy image data are the input data to be virtually colorized by the style-transfer GAN deep learning. In the “ground-truth” data collection, a research-level commercial microscope (NIB900, NOVEL, China) is used under the 10X (NA0.25) magnification objective lens, which is with a halogen lamp. We tried to best align/register the commercial microscopy images with the collected singlet microscopy images by precisely and manually moving the biosample stage, which would help the afterward digital registration greatly. In the deep training stage, the virtual colorization kernels are trained. In this manuscript, we compare the virtual colorization results of blue-LED-illumination singlet microscopy images, green-LED-illumination singlet microscopy images, and red-LED-illumination singlet microscopy images.

Throughout experiments, data collection, deconvolution for a better image contrast, digital registration, and deep training, the virtual colorization results and comparisons are presented in Figs. 4 and 5. In Fig. 4, the blue LED illuminated grayscale image, the green LED illuminated grayscale image, and the red LED illuminated

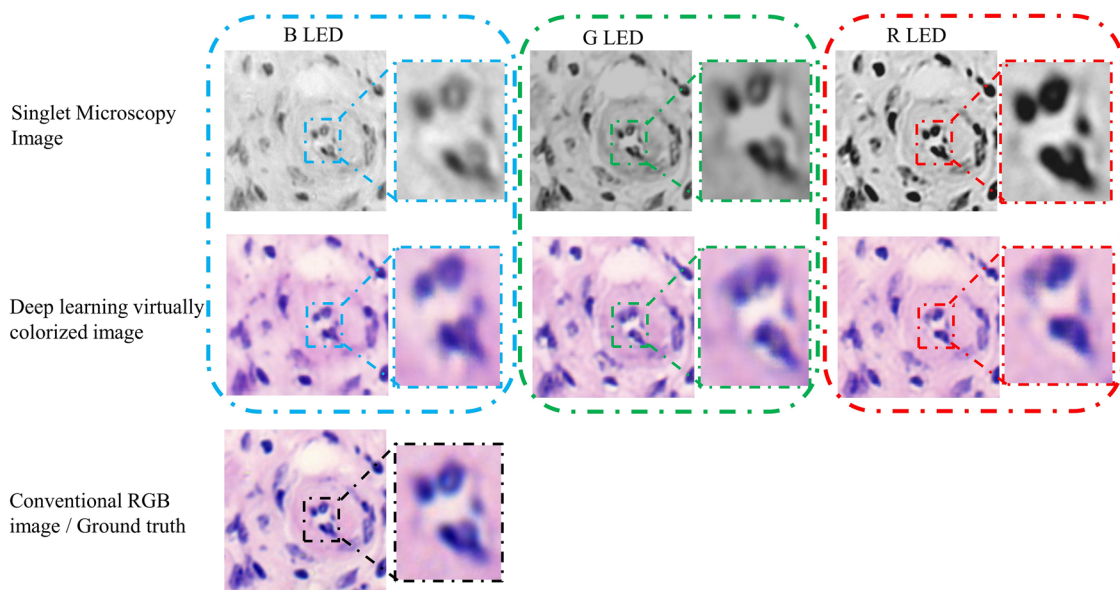


FIG. 4. An example of virtual colorization by deep learning. Differences are presented and zoomed in.

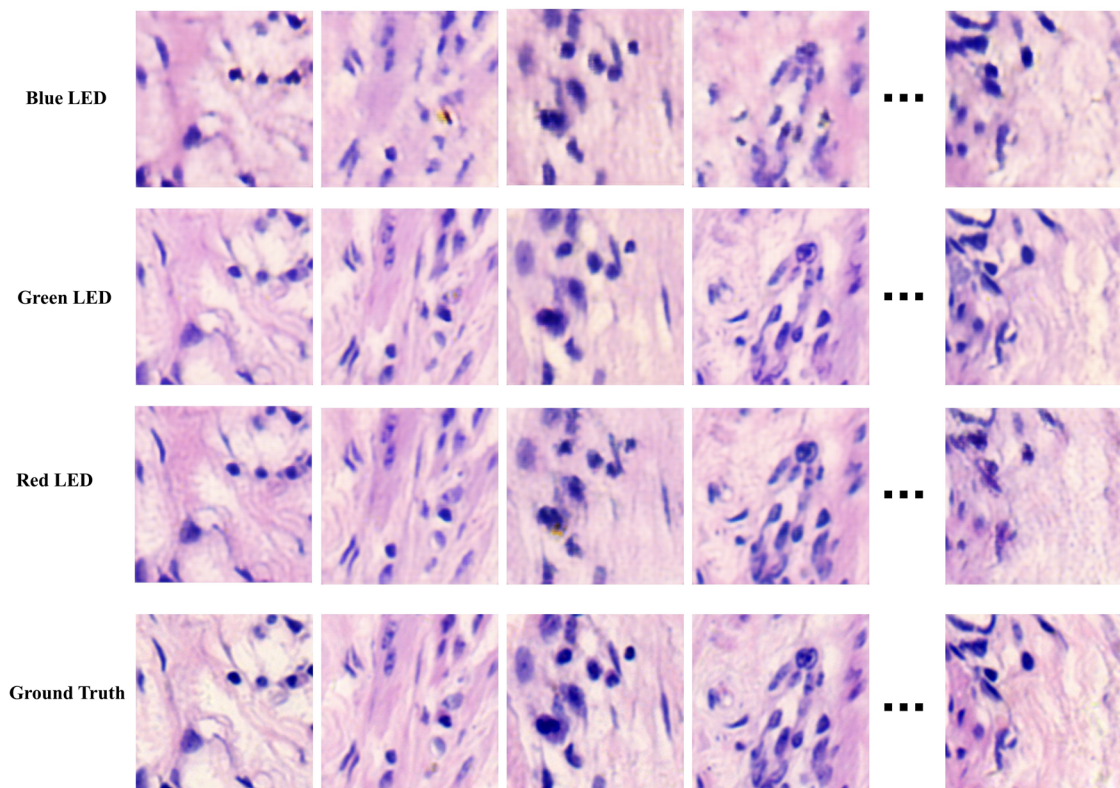


FIG. 5. 200 group images under B/G/R illumination to evaluate the average PSNRs and SSIMs of virtually colorized microscopy images.

TABLE II. PSNRs and SSIMs under the illumination of B LED, G LED, and R LED.

	PSNR	SSIM
B LED	25.906	0.87
G LED	27.590	0.92
R LED	28.610	0.91

grayscale image are presented, which are digitally registered and deconvoluted by the deep learning method²³ to improve the image resolution and image contrast. Comparing the “deep learning virtually colorized images” and the “conventional RGB image/ground truth,” we thought our virtually colorizing deep learning network framework works well. However, in the grayscale images, the different LED illuminated images have different spectral transmission. For example, the red LED illuminated cell nuclear parts are much darker than those in blue LED illuminated images. These differences in spectral transmission caused the image texture differences in grayscale images. Hence, which kind of LED is the best? Thus, we did the comparison data in Fig. 5. In Fig. 5, we tested 200 groups images to calculate the average peak signal noise ratio (PSNR) and structure similarity index measure (SSIM).^{13,14,20} The conventional RGB images are viewed as the criterion when calculating PSNRs and SSIMs, which are presented in Table II. Under blue LED illumination, the PSNR is 25.906 and the SSIM is 0.87. Under green LED illumination, the PSNR is 27.590 and the SSIM is 0.92. Under red LED illumination, the PSNR is 28.610 and the SSIM is 0.91.

In this manuscript, we show a virtual colorful singlet microscopy for H&E stained biosample slides. In the hardware, the illumination is provided by a quasi-chromatic LED, and a singlet aspheric lens is used, which has linear signal properties across all FOVs. In the algorithms, we designed a deep learning GAN framework to achieve virtual colorization. Besides, we compared the virtual colorizing results by transferring three kinds of quasi-chromatic grayscale images. For H&E stained pathological tissue slides, the green LED illumination and the red LED illumination would provide a better PSNR and SSIM than the blue LED illumination. Furthermore, the virtual colorizing methods are also fit for other singlet microscopy situations and other chromatic aberration imaging systems, such as a conventional spherical lens, diffractive lens, and meta-surface lens. Besides, in other chromatic/quasi-chromatic illumination biomedical microscopy imaging applications,^{27–33} such as LED-illumination Fourier ptychographic microscopy (FPM)^{30,31} and laser-illumination quantitative phase microscopy,^{28,29,32,33} our deep learning virtual colorization method could also have the potential to transfer grayscale images to visually comfortable RGB color images.

ACKNOWLEDGMENTS

This study was partially supported by the Basic Research Program of Jiangsu Province (Grant Nos. BK20190456 and BK20201305), the National Natural Science Foundation of China (NSFC, Grant No. 62005120), the Fundamental Research Funds for the Central Universities (Grant No. 30919011261), Beijing

Satellite Environmental Engineering Institute (Grant No. CAST-BISEE2019-038), The Chinese Academy of Sciences (Grant No. KLOMT190101), the Suzhou Science and Technology Development Project (Grant No. SYSD2020132), and the National Key Research and Development Program (Grant No. 2019YFB2005500).

All authors declare that they have no conflict of interest.

DATA AVAILABILITY

The data that support the findings of this study are available from the corresponding author upon reasonable request.

REFERENCES

- G. Muyo, A. Singh, M. Andersson, D. Huckridge, A. Wood, and A. R. Harvey, *Opt. Express* **17**(23), 21118 (2009).
- F. Languy, K. Fleury, C. Lenaerts, J. Loicq, D. Regaert, T. Thibert, and S. Habraken, *Opt. Express* **19**(S3), A280 (2011).
- R. G. González-Acuña and H. A. Chaparro-Romo, *Appl. Opt.* **57**(31), 9341 (2018).
- J. Nagar, S. D. Campbell, and D. H. Werner, *Optica* **5**(2), 99 (2018).
- A. M. Hanninen and E. O. Potma, *APL Photonics* **4**(8), 080801 (2019).
- J. Chen, J. Rao, D. Lisevych, and Z. Fan, *Appl. Phys. Lett.* **114**(10), 104101 (2019).
- X. Wan, W. Xiang Jiang, H. Feng Ma, and T. Jun Cui, *Appl. Phys. Lett.* **104**(15), 151601 (2014).
- Y. Peng, Q. Sun, X. Dun, G. Wetzstein, W. Heidrich, and F. Heide, *ACM Trans. Graphics* **38**(6), 219 (2019).
- D. Xiong, H. Ikoma, W. Gordon, Z. Wang, X. Cheng, and Y. Peng, *Optica* **7**(8), 913 (2020).
- H. Liu, Z. Fu, J. Han, L. Shao, and H. Liu, *J. Visual Commun. Image Representation* **53**, 20 (2018).
- M. T. Shaban, C. Baur, N. Navab, and S. Albarqouni, [arXiv:1804.01601](https://arxiv.org/abs/1804.01601) (2018).
- M. Izadyyazdanabadi, E. Belykh, X. Zhao, L. Borba Moreira, S. Gandhi, C. Cavallo, J. Eschbacher, N. Peter, M. C. Preul, and Y. Yang, [arXiv:1905.06442](https://arxiv.org/abs/1905.06442) (2019).
- R. Yair, T. Liu, Z. Wei, Y. Zhang, K. de Haan, and A. Ozcan, *Light: Sci. Appl.* **8**(1), 23 (2019).
- R. Yair, H. Wang, Z. Wei, K. de Haan, Y. Zhang, Y. Wu, H. Günaydin, J. E. Zuckerman, T. Chong, A. E. Sisk, L. M. Westbrook, W. Dean Wallace, and A. Ozcan, *Nat. Biomed. Eng.* **3**(6), 466 (2019).
- T. Abraham, A. Shaw, D. O'Connor, A. Todd, and R. Levenson, [arXiv:2008.08579](https://arxiv.org/abs/2008.08579) (2020).
- K. de Haan, Y. Rivenson, Y. D. Wu, and A. Ozcan, *Proc. IEEE* **108**(1), 30 (2020).
- H. Liang, K. N. Plataniotis, and X. Li, [arXiv:2007.12578](https://arxiv.org/abs/2007.12578) (2020).
- D. Mahapatra, B. Bozorgtabar, J.-P. Thiran, and L. Shao, [arXiv:2008.02101](https://arxiv.org/abs/2008.02101) (2020).
- H. Nishar, N. Chavanke, and N. Singhal, [arXiv:2010.02659](https://arxiv.org/abs/2010.02659) (2020).
- Y. Rivenson, K. de Haan, W. D. Wallace, and A. Ozcan, *BME Front.* **2020**, 9647163.
- H. Touvron, M. Douze, M. Cord, and H. Jégou, [arXiv:2008.05763](https://arxiv.org/abs/2008.05763) (2020).
- Z. Zuo, Q. Xu, H. Zhang, Z. Wang, H. Chen, A. Li, L. Zhao, W. Xing, and D. Lu, [arXiv:2008.03529](https://arxiv.org/abs/2008.03529) (2020).
- H. Shen and J. Gao, *J. Biophotonics* **13**(6), e202000013 (2020).
- M. Akif Beg and J. Yuan Yu, [arXiv:2003.02909](https://arxiv.org/abs/2003.02909) (2020).
- M. Peško and T. Trzciński, [arXiv:1809.01726](https://arxiv.org/abs/1809.01726) (2018).
- Z. Zou, T. Shi, S. Qiu, Y. Yuan, and Z. Shi, [arXiv:2011.08114](https://arxiv.org/abs/2011.08114) (2020).
- S. Montresor, M. Tahon, A. Laurent, and P. Picart, *APL Photonics* **5**(3), 030802 (2020).
- J. Qian, S. Feng, T. Tao, Y. Hu, Y. Li, Q. Chen, and C. Zuo, *APL Photonics* **5**(4), 046105 (2020).

²⁹J. K. Zhang, Y. R. He, N. Sobh, and G. Popescu, *APL Photonics* **5**(4), 040805 (2020).

³⁰A. Pan, C. Zuo, Y. Xie, L. Lei, and B. Yao, *Opt. Lasers Eng.* **120**, 40 (2019).

³¹A. Pan, C. Zuo, and B. Yao, *Rep. Prog. Phys.* **83**(9), 096101 (2020).

³²J. Zhu, R. Zhou, L. Zhang, B. Ge, C. Luo, and L. L. Goddard, *Opt. Express* **27**(5), 6719 (2019).

³³J. Dou, Z. Gao, J. Ma, C. Yuan, Z. Yang, D. Claus, and T. Zhang, *Appl. Phys. B* **123**(8), 217 (2017).